THE ASTROPHYSICAL JOURNAL, 479:303–306, 1997 April 10

CIRRUS COLOR VARIATIONS DUE TO ENHANCED RADIATION FIELDS

SEAN J. CAREY,[1] R. F. SHIPMAN, AND F. O. CLARK
Department of the Air Force, Geophysics Directorate, Phillips Laboratory, GPOB, 29 Randolph Road, Hanscom AFB, MA 01731-3010

AND

ROB ASSENDORP
Astrophysikalisches Institut Potsdam, An der Sternwarte 16, D-14482 Potsdam-Babelsberg, Germany
Received 1996 May 9; accepted 1996 October 31

ABSTRACT

We have investigated the variations in 12/100, 25/100, 60/100, and 12/25 μm colors for seven main-sequence B stars and three F and G supergiants associated with infrared cirrus. All sources displayed an increase in 60/100 color above the background cirrus color. In two of the sources, ϵ Apodis and HR 890, the 12/100 and 25/100 colors decline toward the embedded star in a similar fashion to the IR colors of S264 and the Rosette Nebula. Current grain models composed of equilibrium-heated submicron grains, transiently heated small grains, and polycyclic aromatic hydrocarbons cannot account for the color variations observed around ϵ Aps and HR 890. The supergiants exhibited 12/100 and 25/100 increases, suggesting that the color deficits observed for the B stars are due to an enhancement in the soft UV component of the radiation field only. A candidate explanation for the color variations is a conglomerate small grain component, composed of very small grains and/or large molecules, that is fragmented in the enhanced radiation field around ϵ Aps and HR 890.

Subject headings: dust, extinction — infrared: ISM: continuum

1. INTRODUCTION

Observations of the infrared colors of diffuse infrared cirrus clouds (Low et al. 1984) provide valuable information on the size distribution and composition of interstellar dust. Detailed studies of the infrared properties of cirrus clouds have been conducted by Laureijs (1989) and Heiles, Reach, & Koo (1988). The infrared emission from cirrus clouds is primarily due to reprocessing of the ambient radiation field by the dust.

A good laboratory for examining interstellar dust is a cirrus cloud heated by an embedded B star. Embedded B stars generally have wandered into the cirrus (Gaustad & Van Buren 1993), and the dust composition is not affected by additional material from the embedded object. The ambient radiation field can be well characterized, and the effects of an enhanced radiation field upon the dust emission properties can be studied.

Shipman & Clark (1994) and Shipman (1994) have investigated the infrared properties of the H II regions: S264 and the Rosette Nebula. Both objects exhibit a decline in 25 μm emission relative to both 12 and 100 μm emission toward the exciting O stars. A similar decline with increased radiation field is noted in the Pleiades star cluster, a collection of main-sequence and giant B stars (Carey, Shipman, & Clark 1997). The decrease in 25 μm emission relative to both 12 and 100 μm in an increased radiation field is difficult to explain with equilibrium (e.g., Draine & Lee 1984; Hong & Greenberg 1980; Mathis, Rumpl, & Nordseik 1977) and stochastically heated (Draine & Anderson 1985) grains, even after accounting for the proposed contribution to short-wavelength emission due to polycyclic aromatic hydrocarbons (PAHs) (see Puget & Léger 1989 and references therein).

We have examined seven main-sequence stars, with spectral types between B1.5 and B9, and three F and G supergiants embedded in infrared cirrus structures to investigate the infrared emission and dust properties as a function of ambient radiation field. In particular, we are interested in determining if the 12 and 25 μm deficits noted for H II regions are present in the vicinity of late-type stars. To this end, we examine the infrared colors of the associated cirrus as a function of stellar spectral type and distance from the embedded object.

2. DATA

The B stars examined were taken from the IR hot spot list of Gaustad & Van Buren (1993), while the supergiants are from Dring et al. (1996). These catalogs consist of stars from the Bright Star Catalog (Hoffleit 1982) with associated infrared emission. Pertinent stellar data is displayed in Table 1. Distances to all stars were estimated by spectroscopic parallax using B and V magnitudes from the SIMBAD database.

We have analyzed the *IRAS* photometric data at 12, 25, 60, and 100 μm using the *IRAS* Sky Survey Atlas (ISSA) data product (Wheelock et al. 1994). A $2^\circ \times 2^\circ$ subimage around each embedded source was created and analyzed. All B stars appeared as distinct bright spots at 60 μm and enhanced patches of 100 μm emission with respect to nearby cirrus. In general, enhancements in the 12 and 25 μm emission were coincident with the 60 μm peak, and the morphology of the emission was similar at all wavelengths. The supergiants showed enhancements at 12 and 25 μm with nearby diffuse emission at 60 and 100 μm.

We have adopted stringent criteria upon the background IR emission for the B stars in order to minimize the contribution of other sources to the infrared emission. All B stars are greater than 20° from the ecliptic plane and 5° from the Galactic plane. Stringent criteria were not applied to the

[1] National Research Council Research Associate.

TABLE 1

SOURCE LIST

Name	R.A. (1950)	Decl. (1950)	Spectral Type	A_v[a]	Distance[b]	r_{equal}[c]
ϵ Aps	14 16 13.1	−79 52 48.4	B4 V	0.3	215	11.5
HR 890	2 57 17.5	52 09 16.1	B7 V	0.4	121	9.5
HR 241	0 48 41.8	51 17 58.7	B9 V	0.2	146	4.5
HR 189	0 41 39.0	47 35 25.8	B5 V	0.2	221	8.5
HR 533	1 48 41.3	54 54 03.0	B1.5 V	0.3	402	19.5
HR 1719.....	5 15 08.6	58 03 57.7	B5 V	0.5	236	8.5
HR 7030.....	18 39 48.0	31 34 05.7	B8 V	0.2	200	4.5
HR 7570.....	19 49 55.5	0 52 33.2	F6 Iab	0.0	677[d]	17.5
HR 8232.....	21 28 55.6	−05 47 31.7	G0 Ib	0.2	661	17.5
HR 9003.....	23 43 32.9	46 08 33.6	G5 Ib	0.1	1458	7.5

NOTE.—Units of right ascension are hours, minutes, and seconds, and units of declination are degrees, arcminutes, and arcseconds.

[a] Calculated using intrinsic colors of Lang 1991 and $R_v = 3.01$ (Whittet 1992).

[b] In parsecs, determined by spectroscopic parallax.

[c] Angular size of region around star in arcminutes, for which the contribution to the radiation field from the star is equal to or greater than the ISRF.

[d] Distance from Dring et al. 1996.

selection of supergiants since only three such stars are listed in Dring et al. (1996).

To account for zero-point offsets in the *IRAS* data and foreground/background emission, we have subtracted a DC background level from each subimage. This simple correction is sufficient since the backgrounds for each source are reasonably uniform. In addition, a DC correction factor will only change the magnitude of any variations in color ratios, but not the shape of the trend, and therefore it cannot substantially bias our conclusions. The background level removed was the minimum pixel value in the 2° × 2° image.

For each offset-corrected set of images, maps of the 12/100, 25/100, 60/100, and 12/25 color ratios were made by calculating a pixel-to-pixel ratio of the image data. Uncertainty maps for each ratio were also calculated by propagating the statistical uncertainty in each map. To examine the variations in infrared colors as a function of distance from the exciting source, each map was azimuthally averaged in

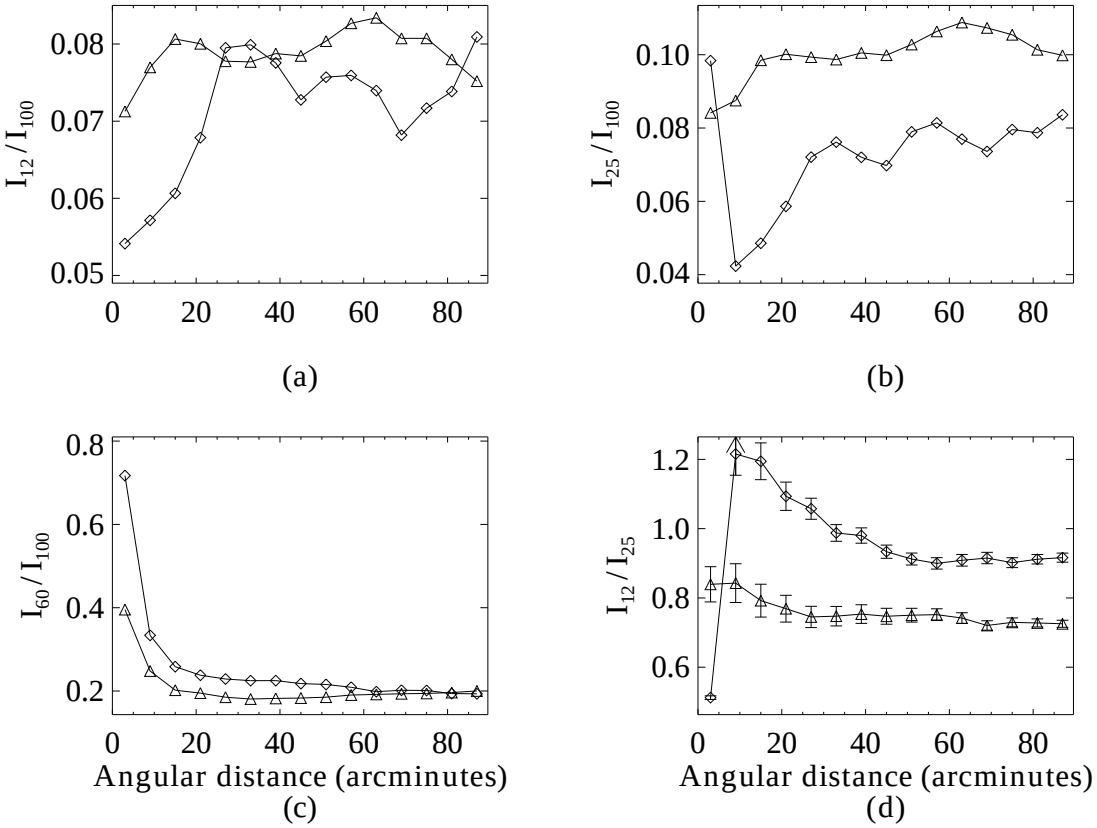

FIG. 1.—Ratio of *IRAS* passband flux densities averaged over annuli of 6′ width for ϵ Aps (*diamonds*) and HR 890 (*triangles*). The annuli are centered on ($14^h16^m17^s$, −79°52′48″.4) for ϵ Aps and on ($2^h57^m17^s$, +52°9′14″.5) for HR 890; 6′ corresponds to 0.38 pc at the distance of ϵ Aps (spectral type B4 V) and 0.21 pc at the distance of HR 890 (B7 V). The 1 σ uncertainties for each point are displayed when the error bars are larger than the data symbols. (*a*) 12/100; (*b*) 25/100; (*c*) 60/100; and (*d*) 12/25.

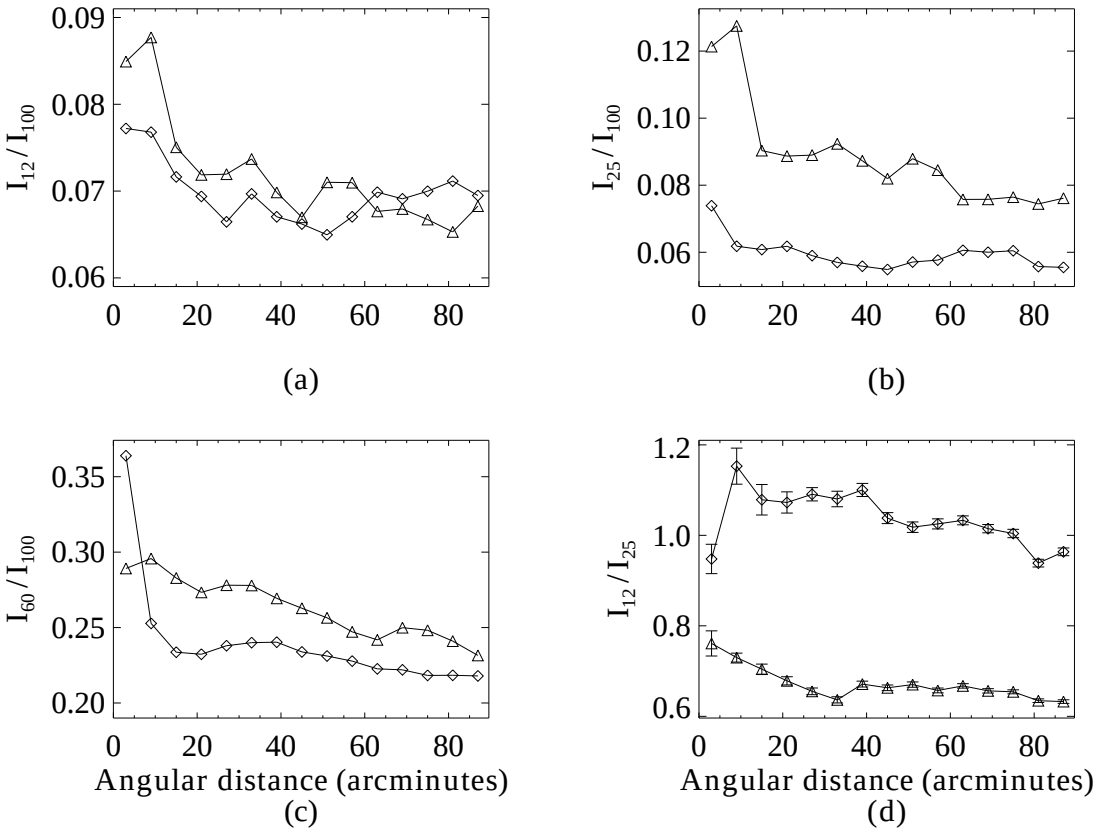

FIG. 2.—Ratio of *IRAS* passband flux densities averaged over annuli of 6′ width for HR 1719 (*diamonds*) and HR 7570 (*triangles*). The annuli are centered on ($5^h15^m09^s$, +58°03′57.″7) for HR 1719 and on ($19^h49^m56^s$, 0°52′33.″2) for HR 7570; 6′ corresponds to 0.41 pc at the distance of HR 1719 (B5 V) and 1.18 pc at the distance of HR 7570 (F6 Iab). The 1 σ uncertainties for each point are displayed when the error bars are larger than the data symbols. (*a*) 12/100; (*b*) 25/100; (*c*) 60/100; (*d*) 12/25.

annuli 1 pixel wide and centered on the coordinates of the exciting star. Each average was then smoothed to 6′, approximately the resolution of ISSA plates at 100 μm.

3. DESCRIPTION OF COLOR VARIATIONS

While the morphology of the infrared emission and the variation in the 12/100, 25/100, and 12/25 infrared colors varied considerably from source to source, all sources (except HR 8232) displayed a peak in the 60/100 color at the position of the exciting star. The supergiants show increased 12/100, 25/100, and 60/100 colors toward the star because of the enhanced heating of interstellar and circumstellar material near the star. The magnitude of the 60/100 peak for the B stars is correlated with spectral type and distance. The 60/100 colors for the B stars decrease smoothly from the peak to the background cirrus value (0.2; Laureijs 1989).

For two of the B stars, ϵ Apodis and HR 890, the 12/100 and 25/100 colors decline toward the star. These variations are similar to those observed in H II regions (Cox, Deharveng, & Leene 1990; Shipman 1994). The 12/25 color for ϵ Aps exhibits complex behavior, reaching a maximum 9′ from the star and then decaying to the background value 40′ away. The remaining B stars show a variety of 12/100 and 25/100 profiles from increasing to slightly decreasing toward the embedded star. All profiles show small-scale fluctuations that are not due to image noise. These variations are due to real structure in the infrared cirrus, as noted by Heiles et al. (1988).

From this data set, it is difficult to determine how common color deficits around B stars are. It is quite possible that deficit regions exist around the remaining B stars but are unresolved because of a combination of later spectral types and larger distances, or because the regions are masked by background emission. One measure of the region of influence of a star is $r_{\rm equal}$, which is the angular size of the region in which the radiation field is equal to or greater than the interstellar radiation field (ISRF; Mathis, Mezger, & Panagia 1983). As shown in Table 1, of the B stars, only HR 533 has a larger $r_{\rm equal}$ than ϵ Aps and HR 890. However, HR 533 also has the most complicated background (as determined by visual inspection) of all the B stars studied.

The supergiants studied show 12/100 and 25/100 increasing toward the stars. By comparing the color variations of the supergiants with the B stars, we are able to examine the relative importance of the hardness and energy density of the radiation field to the observed color deficits. The color deficits were observed only for the B stars, indicating that an enhancement in the UV radiation field is the cause of the observed 12/100 and 25/100 color deficits. This conclusion is reasonable since the small grains responsible for most of the emission at 12 and 25 μm are preferentially heated by UV photons (Puget & Léger 1989). However, the radiation field of ϵ Aps is not significantly harder than the interstellar radiation field, and HR 890 is even softer. From our limited data set, we conjecture that an enhancement in the soft UV component of the radiation field is sufficient to produce the observed color deficits around ϵ Aps and HR 890, as well as the UV-rich environments of S264 and the Rosette Nebula. The color profiles of ϵ Aps and HR 890 are shown in Figure

1, while the profiles of one of the supergiants (HR 7570) and a B star not showing a deficit (HR 1719) are displayed for comparison in Figure 2.

4. COLOR DEFICIT MECHANISMS

While the declining 12/100 and 25/100 colors could be explained by the presence of a second, cooler dust component along the line of sight to the embedded star, the increasing 60/100 color for our sources rules out this possibility. The declining 12/100 and 25/100 colors in the presence of an enhanced radiation field cannot be explained by the equilibrium heating of classical grains. Current emission models (Lis & Leung 1991; Bernard et al. 1992; Shipman 1994) for transiently heated small grains indicate that the 12/100 and 25/100 colors increase in the presence of an enhanced radiation field since the larger density of UV photons is responsible for increased emission by the stochastically heated very small grains. No standard grain emission model consisting of classical silicate and graphite grains, small transiently heated grains, and PAHs can explain the decline in 12/100 and 25/100 color observed for ϵ Aps and HR 890.

Grain destruction can possibly account for the declining 12 and 25 μm emission. In an enhanced UV radiation field, the smallest grains will be destroyed first (Guhathakurta & Draine 1989). The remaining large grains will be heated by the enhanced radiation field as evidenced by the 60/100 color peak. While grain destruction may explain the infrared colors of HR 890, the peak in the 12/25 color for ϵ Aps cannot be explained simply by the destruction of small grains. The majority of 12 μm emission is predicted to come from grains smaller than the grains responsible for the bulk of the 25 μm emission; therefore, if grain destruction is responsible, then the process must preferentially destroy the carriers of 25 μm emission over those emitting at 12 μm.

Small grains, which are conglomerates of either large molecules or smaller grains weakly bound together, are a possible carrier for the 25 μm emission (Clark et al. 1995). Weak bonds between the subunits (large molecules and/or smaller grains) could be broken by the enhanced UV radiation in the vicinity of the star. The fragmentation of the conglomerate grains may replenish the very small grains responsible for the bulk of the 12 μm emission, partially offsetting the photodestruction of the 12 μm carriers. In this scenario, the decline in 12/100 and 25/100 colors is explained by destruction and conversion of the small grains as the star is approached. The rise in 12/25 is caused by the shattering of conglomerate grains, producing enough 12 μm emitters to partially offset the destruction of very small grains, and the minimum in 12/25 is the result of the destruction of most of the very small grains by the UV radiation field of the star. The unresolved, central 25/100 peak may be explained by heating of the remaining classical grains to temperatures in excess of 39 K (observed 25/100 color temperature) close to the star.

5. SUMMARY

We have examined the infrared color variations of seven main-sequence B stars and three late-type supergiants embedded in interstellar cirrus. All three supergiants show increasing 12/100, 25/100, and 60/100 colors as the embedded star is approached. The B stars have increasing 60/100 colors approaching the stars, as predicted by standard grain emission models. Two of the B stars, ϵ Aps and HR 890, show decreasing 12/100 and 25/100 colors toward the star. This is contrary to the predictions of current grain emission models in the presence of an enhanced radiation field. One interpretation of this effect is that the small grains are destroyed by the enhanced UV radiation field in the vicinity of a B star. The deficiency of 25 μm emission relative to 12 μm around ϵ Aps suggests that the 25 μm carriers are conglomerates that are fragmented by the UV radiation field.

This work was performed while S. J. C. held a National Research Council–AFGL Research Associateship. This research has made use of the SIMBAD database, operated at CDS, Strasbourg, France.

REFERENCES

Bernard, J. P., Boulanger, F., Desért, F. X., & Puget, J. L. 1992, A&A, 263, 258
Carey, S. J., Shipman, R. F., & Clark, F. O. 1997, in From Stardust to Planetesimals, ed. M. E. Kress, A. G. G. M. Tielens, & Y. Pendleton (CP-3343; Washington, DC: NASA)
Clark, F. O., Shipman, R. F., Assendorp, R., Kester, D., & Egan, M. P. 1995, Planet. Space Sci., 43, 1353
Cox, P., Deharveng, L., & Leene, A. 1990, A&A, 230, 181
Draine, B. T., & Anderson, N. 1985, ApJ, 292, 494
Draine, B. T., & Lee, H. M. 1984, ApJ, 285, 89
Dring, A. R., Murthy, J., Henry, R. C., & Walker, H. J. 1996, ApJ, 457, 764
Gaustad, J. E., & Van Buren, D. 1993, PASP, 105, 1127
Guhathakurta, P., & Draine, B. T. 1989, ApJ, 345, 230
Heiles, C., Reach, W. T., & Koo, B. C. 1988, ApJ, 332, 313
Hoffleit, D. 1982, Catalog of Bright Stars (4th ed.; New Haven: Yale Univ. Obs.)
Hong, S. S., & Greenberg, J. M. 1980, A&A, 88, 194
Lang, K. R. 1991, Astrophysical Data: Planets and Stars (New York: Springer)
Laureijs, R. J. 1989, Ph.D. thesis, Univ. Groningen
Lis, D. C., & Leung, C. M. 1991, ApJ, 372, L107
Low, F. J., et al. 1984, ApJ, 278, L19
Mathis, J. S., Mezger, P. G., & Panagia, N. 1983, A&A, 128, 212
Mathis, J. S., Rumpl, W., & Nordseik, K. H. 1977, ApJ, 217, 425
Puget, J. L., & Léger, A. 1989, ARA&A, 27, 167
Shipman, R. F. 1994, Ph.D. thesis, Univ. Wyoming
Shipman, R. F., & Clark, F. O. 1994, ApJ, 422, 153
Wheelock, S. L., et al. 1994, *IRAS* Sky Survey Atlas Explanatory Supplement (JPL Publ. 94-11; Pasadena: JPL)
Whittet, D. C. B. 1992, Dust in the Galactic Environment (Bristol: IoPP)